

# Pseudo-static Analysis of Reinforced Earth Retaining Wall considering Non-linear Failure Surface

Sima Ghosh · Chirabrata Debnath

Received: 9 April 2013 / Accepted: 18 April 2016 / Published online: 6 May 2016  
© Springer International Publishing Switzerland 2016

**Abstract** The seismic stability of reinforced earth has been investigated in this paper using pseudo-static method of analysis considering horizontal and vertical seismic acceleration with non-linear failure surface. The sliding wedge is divided into a number of horizontal slices to determine the strength and length of the geo-synthetic reinforcement for seismic internal stability of battered face rigid retaining wall supporting  $c$ - $\Phi$  backfill. Results are presented in graphical form representing the required length of geo-synthetic reinforcement under seismic condition to maintain the internal stability of reinforced soil. The influences of horizontal and vertical seismic acceleration, soil friction angle, cohesion, adhesion and wall inclination angle on the required length of the geo-synthetic reinforcement have been studied. From the present study it is seen that the required length of geo-synthetic reinforcement increases due to increase in the value of seismic accelerations.

**Keywords** Pseudo-static · Tensile strength · Length of geo-synthetic reinforcement · Horizontal slice method · Reinforced  $c$ - $\Phi$  backfill · Non-linear failure surface

## List of symbols

$\theta_1$	Failure surface angle with vertical for top slice
$\theta_n$	Failure surface angle with vertical for bottom slice
$\theta_R$	Rate of change of failure surface angle
$\Phi$	Soil friction angle
$\delta_r = \Phi$	Angle of friction between reinforcing strips and soil
$c$	Cohesion
$c_a$	Adhesion
$N_c$	$(\Delta H/H) * N_s$
$M_c$	$(\Delta H/H) * M_s$
$\alpha$	Wall inclination angle with the vertical
$k_h$	Horizontal seismic acceleration co-efficient
$k_v$	Vertical seismic acceleration co-efficient
$\Delta H$	Height of each slice
$W_i$	Weight of $i$ th slice
$R$	Soil reaction force
$V_1$	Vertical load (UDL) acting on the bottom surface of the 1st layer
$V_2$	Vertical load (UDL) acting on the top surface of the 1st layer
$\gamma$	Unit weight of soil
$b$	Width of reinforcing strip
$Z_i$	Depth of reinforcing strip in $i$ th layer
$F_i$	Frictional resistance force on the reinforcing strip
$t_i$	Required geo-synthetic tensile reinforcement force of the $i$ th layer

S. Ghosh (✉) · C. Debnath  
Civil Engineering Department, National Institute of  
Technology Agartala, Agartala, Tripura 799046, India  
e-mail: sima.civil@nita.ac.in

$L_{ei}$	Effective length of reinforcement of $i$ th layer
$L_t$	$\sum L_{ei} + \sum L_i$

### 1 Introduction

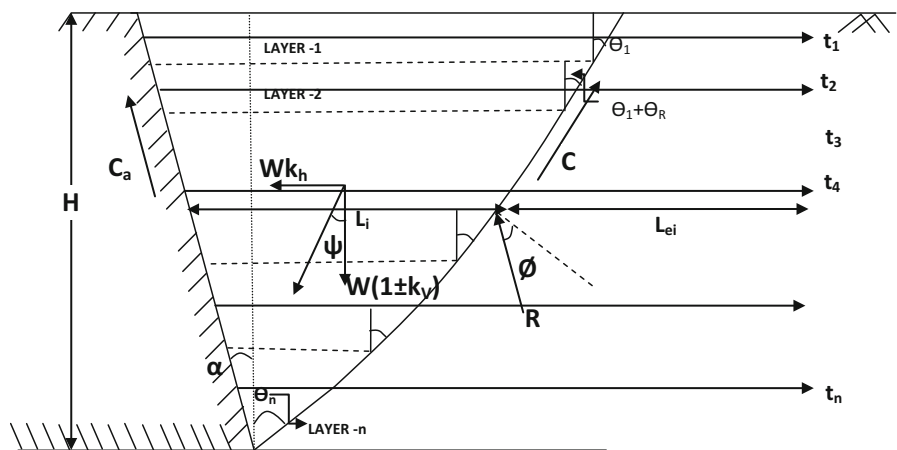
The design of reinforced earth under seismic condition is one of the most important topic in Geotechnical Engineering field. The advantageous feature of reinforced earth is that the reinforcements restrain the lateral earth pressure acting on the wall due to the development of soil reinforcement interface frictional force. A number of investigations have been performed by several researchers to predict the seismic internal stability of reinforced soil under earthquake loading. Mononobe-Okabe (1926; Mononobe and Matsuo 1929) first established the solution for seismic earth pressure by incorporating the seismic acceleration as inertia force in classical Coulomb's theory. Ling et al. (1997) have analyzed the seismic stability of reinforced soil wall based on pseudo-static limit equilibrium analysis, which considers only the horizontal seismic acceleration in the soil medium. Ling and Leshchinsky (1998) have also studied the effect of vertical and horizontal seismic accelerations on the required strength and length of reinforcement layers. Shahgholi et al. (2001) using horizontal slice method (HSM) and assuming multilinear failure plane determined the required tensile force generated in a reinforced soil wall subjected to both horizontal and vertical seismic forces. Nouri et al. (2008) evaluated

the effects of the horizontal and vertical seismic acceleration on reinforced soil slopes and walls using Horizontal Slices Method. Nimbalkar et al. (2006) analyzed the seismic stability of reinforced soil wall by considering the pseudo-dynamic approach. Ghosh and Datta (2012) determined passive force on retaining wall under static loading condition supporting  $\Phi$  backfill using horizontal slice method with curvilinear rupture surface. Ghosh and Saha (2013) evaluated active earth pressure again using non-linear rupture surface under static loading condition. Ghosh and Saha (2014) also analyzed pseudo-dynamic passive resistance of a battered-faced retaining wall supporting  $c-\Phi$  backfill with a non-linear failure surface. In the present analysis, an effort has been made to determine the required geo-synthetic tensile reinforcement force and required length of geosynthetic reinforcement to maintain the internal stability of reinforced  $c-\Phi$  soil wall by applying Horizontal Slices Method and considering non-linear failure surface.

### 2 Method of Analysis

Consider a reinforced soil wall of height,  $H$  inclined at an angle  $\alpha$  with the vertical supporting reinforced  $c-\Phi$  backfill and the shape of failure surface is non-linear in nature as shown in Fig. 1. The failure surface makes an angle  $\theta_1$  and  $\theta_n$  with the vertical at bottom and top respectively. Limit equilibrium method and the Horizontal Slice Method are considered to analyze the seismic stability of reinforced soil wall. The sliding

**Fig. 1** Model of reinforced soil wall during active state of equilibrium considering non-linear failure criteria



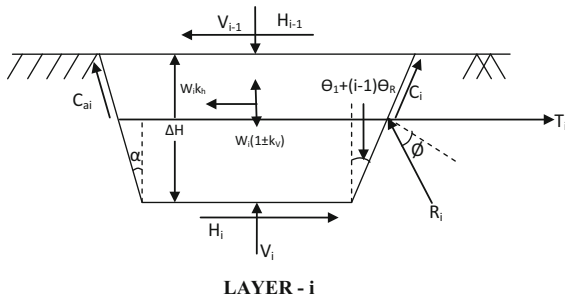


**Fig. 2** Forces acting on *i*th horizontal slice

mass of soil is divided into ‘*n*’ number of horizontal slices each with a layer of reinforcement at its middle. The rate of change of failure angle ( $\theta_1$  and  $\theta_n$ ) has been assumed as  $\theta_r = \{(\theta_1 - \theta_n) / (n - 1)\}$ . Forces acting on single horizontal elemental slice containing reinforcement are shown in Fig. 2.

The following parameters are considered for the calculation of required geosynthetic tensile force:  $W_i$  = Weight of the failure wedge of *i*th slice,  $V_{i-1}$ ,  $V_i$  = Vertical load (UDL) on top and bottom of *i*th slice,  $\Phi$  = angle of internal friction of soil,  $c$  = unit cohesion,  $c_a$  = unit adhesion,  $t_i$  = Required geosynthetic tensile force for *i*th slice,  $R_i$  = Reaction of the retained soil on *i*th slice,  $k_h$  = Horizontal seismic acceleration,  $k_v$  = Vertical seismic acceleration

$$\sum_{i=1}^n t_i - \sum_{i=1}^n R_i \cos(\phi + \theta_1 + (i - 1)\theta_r) - \sum_{i=1}^n \left(i - \frac{1}{2}\right) \gamma \Delta H^2 \{\tan \alpha + \tan(\theta_1 + (i - 1)\theta_r)\} k_h + \sum_{i=1}^n \frac{c \Delta H \sin(\theta_1 + (i - 1)\theta_r)}{\cos(\theta_1 + (i - 1)\theta_r)} - \sum_{i=1}^n \frac{c_a \Delta H \sin \alpha}{\cos \alpha} = 0 \tag{1}$$

For *i*th slice

$$t_i - R_i \cos(\phi + \theta_1 + (i - 1)\theta_r) - \left(i - \frac{1}{2}\right) \gamma \Delta H^2 \{\tan \alpha + \tan(\theta_1 + (i - 1)\theta_r)\} k_h + \frac{c \Delta H \sin(\theta_1 + (i - 1)\theta_r)}{\cos(\theta_1 + (i - 1)\theta_r)} - \frac{c_a \Delta H \sin \alpha}{\cos \alpha} = 0 \tag{2}$$

$$\sum V = 0$$

For *i*th slice

$$\left(i - \frac{1}{2}\right) \gamma \Delta H^2 (\tan \alpha + \tan(\theta_1 + (i - 1)\theta_r)) (1 \pm k_v) - R_i \sin(\phi + \theta_1 + (i - 1)\theta_r) - \frac{c \Delta H \cos(\theta_1 + (i - 1)\theta_r)}{\cos(\theta_1 + (i - 1)\theta_r)} - \frac{c_a \Delta H \cos \alpha}{\cos \alpha} = 0 \tag{3}$$

From Eqs. 2 and 3 and after simplification we get,

$$t_i = \frac{\frac{1}{2} \left[ (\Delta H)^2 (1 \pm k_v) \{ (2i - 1) (\tan \alpha + \tan(\theta_1 + (i - 1)\theta_r)) (\tan \psi \sin(\phi + \theta_1 + (i - 1)\theta_r) + \cos(\phi + \theta_1 + (i - 1)\theta_r)) - \frac{N_s \cos \phi}{\cos(\theta_1 + (i - 1)\theta_r)} - \frac{M_s \cos(\phi + \alpha + \theta_1 + (i - 1)\theta_r)}{\cos \alpha} \} \right]}{\sin(\phi + \theta_1 + (i - 1)\theta_r)} \tag{4}$$

### 2.1 Tensile forces generated in the reinforcement

The required tensile strength of each geo-synthetic reinforcement layer is determined from the pseudo-static method of analysis, using horizontal slices method and considering a non-linear failure surface. Applying the force equilibrium conditions for *i*th slice, we can solve the equations in the following pattern:

$$\sum H = 0$$

For the whole wedge,

$$N_s = \frac{2C}{\gamma \Delta H (1 \pm K_v)} \quad M_s = \frac{2C_a}{\gamma \Delta H (1 \pm K_v)} \Psi = \tan^{-1} \frac{\alpha_h}{1 \pm \alpha_v}$$

The geo-synthetic tensile reinforcement force  $t_i$  required to maintain local stability of *i*th layer can be normalized to a parameter  $T_c$ , which is equivalent to the earth pressure coefficient

$$T_c = \frac{\sum_{i=1}^n t_i}{\frac{1}{2} H^2} \tag{5}$$

The required geo-synthetic tensile force in each layer, in case of reinforced c- $\Phi$  soil gives negative value up to a certain depth from the top of retaining wall indicating that there is no requirement of reinforcement up to that length and this depth increases with the increase in cohesion and adhesion value. In this paper, it is assumed that the total required geo-synthetic tensile reinforcement force is the sum of required positive geo-synthetic tensile force for each layer. The anchorage length of the reinforcing strip for the depth up to tensile crack zone has been provided according to the minimum anchorage length of the reinforcing strip as determined from the positive geo-synthetic tensile force.

### 2.2 Determination of Anchorage Length of Reinforcement

Geo-synthetic reinforcing strip should have adequate anchorage length to mobilize the tension developed in the reinforcement. Let us consider a reinforcing strip at  $i$ th slice, the frictional resistance force on the reinforcing strip of effective length  $L_e$  is given by:

$$F_i = t_i \tag{6}$$

If  $\delta_r$  is the angle of friction between reinforcing strips and soil,

$$F_i = (\gamma \times Z_i) \tan \delta_r \times (\text{surface area of the reinforcing strip}) \tag{7}$$

where  $Z_i$  is the depth reinforcing strip of  $i$ th slice.

The surface area of the strip of width ( $b$ ) equal to ( $2bL_e$ ) considering the resistance force developed on both faces of the strips.

Thus

$$F_i = (\gamma \times Z_i) \times \mu \times \tan \delta_r \times (2bL_e) \tag{8}$$

where  $\mu$  is the soil-reinforcement pullout co-efficient.

Substituting the value of  $F_i$  in Eq. (6) and on simplification

$$L_e = \frac{t_i}{2\gamma Z_i \mu b \tan \delta_r} \tag{9}$$

### 2.3 Parametric Study

A detailed parametric study has been conducted to find the effects of the wide range of variation of parameters like angle of internal friction ( $\Phi$ ), wall inclination

angle( $\alpha$ ), seismic accelerations ( $k_h, k_v$ ), and cohesion, adhesion on the required geo-synthetic tensile force and the required length of geo-synthetic reinforcement strip. Variation of parameters considered is as follows:  $\Phi = 20^\circ, 25^\circ$  and  $30^\circ, \alpha = +20^\circ, 0^\circ$  and  $-20^\circ, k_h = 0, 0.1$  and  $0.2, k_v = 0, k_h/2$  and  $k_h, H = 5$  m,  $b = 0.1$  m,  $\gamma = 18$  kN/m<sup>3</sup>

#### 2.3.1 Effect of Soil Friction Angle ( $\Phi$ ) on Reinforcement Force

The variation of required geo-synthetic tensile reinforcement force co-efficient with respect to horizontal seismic acceleration ( $k_h$ ) at different soil friction angle ( $\Phi$ ) for  $\alpha = 0, k_v = k_h/2$  and  $N_c = 0.222, M_c = N_c$  is shown in Fig. 3. From the plot, it is seen that due to the increase in  $\Phi$ , the required geo-synthetic tensile reinforcement force co-efficient ( $T_c$ ) is going to be decreased. The reason behind it with increase in soil friction angle the magnitude of frictional developed between soil-reinforcement interface is going to be increased and required geo-synthetic tensile reinforcement force co-efficient ( $T_c$ ) decreases. For example, at  $\alpha = 0^\circ, c = 8.99$  kN/m<sup>2</sup>,  $c_a = c$  and  $k_h = 0.2, k_v = k_h/2$  the decrease in required geo-synthetic tensile reinforcement force co-efficient ( $T_c$ ) is 24 % for  $\Phi = 20^\circ$  over  $\Phi = 30^\circ$ .

#### 2.3.2 Effect of Wall Inclination Angle ( $\alpha$ ) on Reinforcement Force

The variation of the required geo-synthetic tensile reinforcement force co-efficient with respect to soil

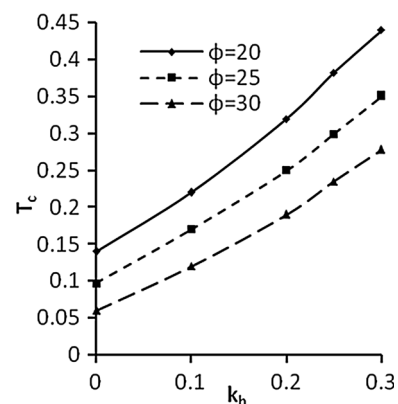


**Fig. 3** Variation of required geo-synthetic tensile reinforcement force co-efficient with respect to horizontal seismic acceleration ( $k_h$ ) at different soil friction angle ( $\Phi$ ) for  $\alpha = 0, k_h = k_h/2$  and  $N_c = 0.222, M_c = N_c$

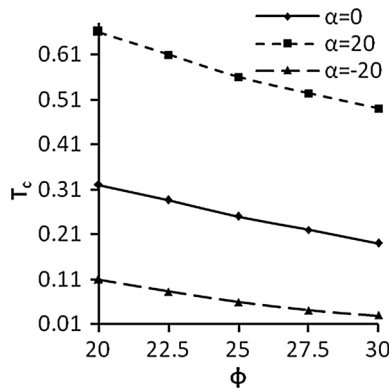


**Fig. 4** Variation of required geo-synthetic tensile reinforcement force co-efficient with respect to soil friction angle ( $\Phi$ ) at different wall inclination angle ( $\alpha$ ) for  $k_h = 0.2$ ,  $k_v = k_h/2$  and  $N_c = 0.222$ ,  $M_c = N_c$

friction angle ( $\Phi$ ) at different wall inclination angle ( $\alpha$ ) for  $k_h = 0.2$ ,  $k_v = k_h/2$  and  $N_c = 0.222$ ,  $M_c = N_c$  is shown in Fig. 4. From the plot it is seen that the magnitude of the required geo-synthetic tensile reinforcement force co-efficient ( $T_c$ ) is going to be increased with the increase in wall inclination angle ( $\alpha$ ). For example, at  $\Phi = 25^\circ$ ,  $k_h = 0.2$ ,  $k_v = k_h/2$  and  $N_c = 0.222$ ,  $M_c = N_c$  the increase in required geo-synthetic tensile reinforcement force co-efficient ( $T_c$ ) is 124 % for  $\alpha = 20^\circ$  over  $\alpha = 0^\circ$ .

**2.3.3 Effect of Horizontal Seismic Acceleration ( $k_h$ ) on Reinforcement Force**

The variation of the required geo-synthetic tensile reinforcement force co-efficient with respect to soil friction angle ( $\Phi$ ) at different horizontal seismic acceleration ( $k_h$ ) for  $\alpha = 0$ ,  $k_v = 0$  and  $N_c = 0.222$ ,  $M_c = N_c$  is shown in Fig. 5. From the plot, it is seen that due to the increase in  $k_h$  value, required geo-synthetic tensile reinforcement force co-efficient ( $T_c$ ) is going to be increased. For example, at  $\Phi = 30^\circ$ ,  $\alpha = 0^\circ$ ,  $N_c = 0.222$ ,  $M_c = N_c$  and  $k_v = k_h/2$  the increase in required geo-synthetic tensile reinforcement force co-efficient ( $T_c$ ) is 58.3 % for  $k_h = 0.2$  over  $k_h = 0.1$ .

**2.3.4 Effect of Vertical Seismic Acceleration ( $k_v$ ) on Reinforcement Force**

The variation of required geo-synthetic tensile reinforcement force co-efficient with respect to horizontal

seismic acceleration ( $k_h$ ) and soil friction angle ( $\Phi$ ) at different vertical seismic acceleration ( $k_v$ ) for  $\alpha = 0$ ,  $k_h = 0.2$  and  $N_c = 0.222$ ,  $M_c = N_c$  is shown in Figs. 6 and 7. From the plot, it is seen that the magnitude of the required geo-synthetic tensile reinforcement force co-efficient ( $T_c$ ) is going to be increased with the increase in vertical seismic acceleration ( $k_v$ ). For example, at  $\Phi = 30^\circ$ ,  $k_h = 0.2$ ,  $N_c = 0.222$ ,  $M_c = N_c$  and  $\alpha = 0^\circ$  the increase in required geo-synthetic tensile reinforcement force co-efficient ( $T_c$ ) is 4.21 % for  $k_v = 1.0 k_h$  over  $k_v = 0.5 k_h$ .

**2.3.5 Effect of Cohesion on Reinforcement Force**

The variation of required geo-synthetic tensile reinforcement force co-efficient with respect to soil

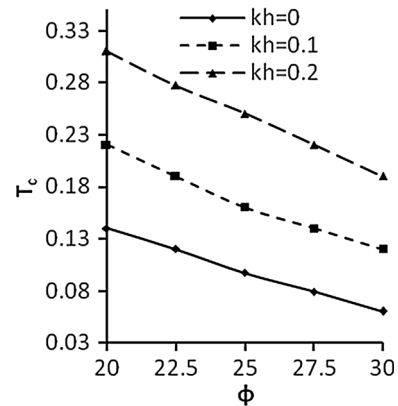


**Fig. 5** Variation of required geo-synthetic tensile reinforcement force co-efficient with respect to soil friction angle ( $\Phi$ ) at different horizontal seismic acceleration ( $k_h$ ) for  $\alpha = 0$ ,  $k_v = 0$  and  $N_c = 0.222$ ,  $M_c = N_c$

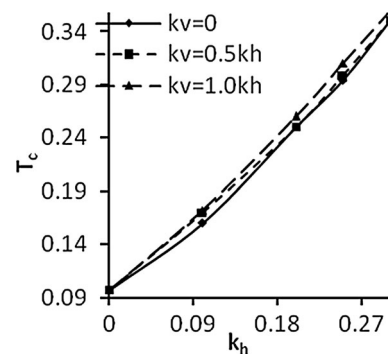


**Fig. 6** Variation of required geo-synthetic tensile reinforcement force co-efficient with respect to horizontal seismic acceleration ( $k_h$ ) at different vertical seismic acceleration ( $k_v$ ) for  $\alpha = 0$ ,  $\Phi = 25$  and  $N_c = 0.222$ ,  $M_c = N_c$

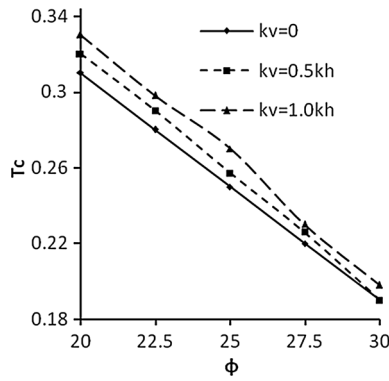


**Fig. 7** Variation of required geo-synthetic tensile reinforcement force co-efficient with respect to soil friction angle ( $\Phi$ ) at different vertical seismic acceleration ( $k_v$ ) for  $\alpha = 0$ ,  $k_h = 0.2$  and  $N_c = 0.222$ ,  $M_c = N_c$

friction angle ( $\Phi$ ) at different  $N_c$  value for  $\alpha = 0$ ,  $k_h = 0.2$ ,  $k_v = k_h/2$  and  $M_c = N_c$  is shown in Fig. 8. From the plot it is seen that the magnitude of required geo-synthetic tensile reinforcement force co-efficient is going to be decreased due to the increase in  $N_c$  value. For example at  $\Phi = 20^\circ$ ,  $\alpha = 0^\circ$ ,  $M_c = N_c$  and  $k_h = 0.2$ ,  $k_v = k_h/2$ , the decrease in  $T_c$  is 55.55 % for  $N_c = 0.222$  over  $N_c = 0$  value whereas  $\Phi = 20^\circ$ ,  $\alpha = 0^\circ$ ,  $M_c = N_c$  and  $k_h = 0.2$ ,  $k_v = k_h/2$ , the decrease in  $T_c$  is 30.56 % for  $N_c = 0.1$  over  $N_c = 0$  value.

**2.3.6 Effect of Soil Friction Angle ( $\Phi$ ) on Required Geo-synthetic Length**

The variation of required length of geo-synthetic reinforcement to height of the wall ratio ( $L_r/H$ ) with respect to horizontal seismic acceleration ( $k_h$ ) at

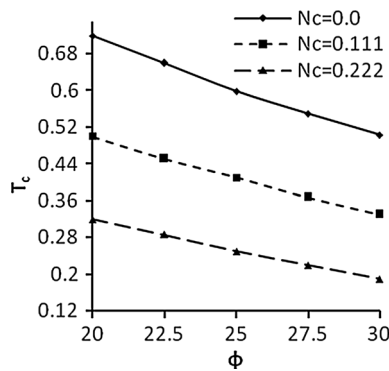


**Fig. 8** Variation of required geo-synthetic tensile reinforcement force co-efficient with respect to soil friction angle ( $\Phi$ ) at different  $N_c$  value for  $\alpha = 0$ ,  $k_h = 0.2$ ,  $k_v = k_h/2$  and  $M_c = N_c$

different soil friction angle ( $\Phi$ ) for  $b = 0.1$ ,  $\alpha = 0^\circ$ ,  $k_v = k_h/2$  and  $N_c = 0.222$ ,  $M_c = N_c$  is shown in Fig. 9. From the plot, it is seen that due to the increase in  $\Phi$ , the required length of geo-synthetic reinforcement to height of the wall ratio ( $L_r/H$ ) is going to be decreased. For example, at  $\alpha = 0^\circ$ ,  $b = 0.1$ ,  $k_h = 0.2$ ,  $k_v = k_h/2$  and  $N_c = 0.222$ ,  $M_c = N_c$  the decrease in required length of geo-synthetic reinforcement to height of the wall ratio ( $L_r/H$ ) is 19.9 % for  $\Phi = 20^\circ$  over  $\Phi = 25^\circ$ .

**2.3.7 Effect of Wall Inclination Angle ( $\alpha$ ) on Required Geo-synthetic Length**

The variation of required length of geo-synthetic reinforcement to height of the wall ratio ( $L_r/H$ ) with respect to soil friction angle ( $\Phi$ ) at different wall inclination angle ( $\alpha$ ) for  $b = 0.1$ ,  $k_h = 0.2$ ,  $k_v = k_h/2$  and  $N_c = 0.222$ ,  $M_c = N_c$  is shown in Fig. 10. From the plot, it is seen that the magnitude of the required length of geo-synthetic reinforcement to height of the wall ratio ( $L_r/H$ ) is going to be increased with the increase in wall inclination angle ( $\alpha$ ). When the inclination of the wall is positive (away from the backfill) earth pressure acting on the wall is higher hence required greater length of geo-synthetic reinforcement than the wall with negative inclination (towards the backfill). The reason behind it is that when the inclination of the wall is positive with the vertical then it has to support more soil in comparison to the wall when it is inclined negative with the vertical. On the other hand, in the case of negative batter as passive earth pressure generates, due to that active earth pressure on the wall is going to be

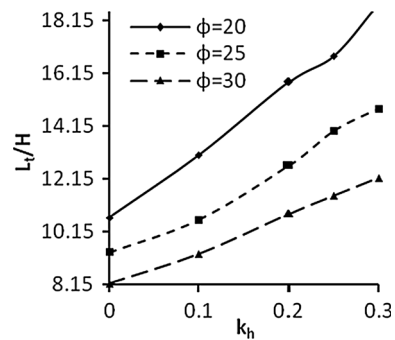


**Fig. 9** Variation of required length of geo-synthetic reinforcement to height of the wall ratio ( $L_r/H$ ) with respect to horizontal seismic acceleration ( $k_h$ ) at different soil friction angle ( $\Phi$ ) for  $b = 0.1$ ,  $\alpha = 0^\circ$ ,  $k_v = k_h/2$  and  $N_c = 0.222$ ,  $M_c = N_c$

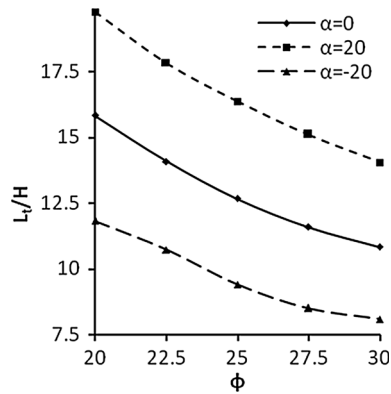


**Fig. 10** Variation of required length of geo-synthetic reinforcement to height of the wall ratio ( $L_r/H$ ) with respect to soil friction angle ( $\Phi$ ) at different wall inclination angle ( $\alpha$ ) for  $b = 0.1$ ,  $k_h = 0.2$ ,  $k_v = k_h/2$  and  $N_c = 0.222$ ,  $M_c = N_c$

reduced. For example, at  $\Phi = 30^\circ$ ,  $b = 0.1$ ,  $k_h = 0.2$ ,  $k_v = k_h/2$  and  $N_c = 0.222$ ,  $M_c = N_c$  the increase in required length of reinforcement to height of the wall ratio ( $L_r/H$ ) is 29.7 % for  $\alpha = 20^\circ$  over  $\alpha = 0^\circ$ .

**2.3.8 Effect of Horizontal Seismic Acceleration ( $k_h$ ) on Required Geo-synthetic Length**

The variation of required length of geo-synthetic reinforcement to height of the wall ratio ( $L_r/H$ ) with respect to soil friction angle ( $\Phi$ ) at different horizontal seismic acceleration ( $k_h$ ) for  $b = 0.1$ ,  $\alpha = 0^\circ$ ,  $k_v = 0$  and  $N_c = 0.222$ ,  $M_c = N_c$  is shown in Fig. 11. From the plot, it is seen that due to the increase in  $k_h$ , the required length of geo-synthetic reinforcement to

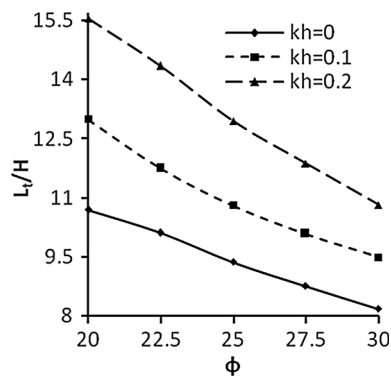


**Fig. 11** Variation of required length of geo-synthetic reinforcement to height of the wall ratio ( $L_r/H$ ) with respect to soil friction angle ( $\Phi$ ) at horizontal seismic acceleration ( $k_h$ ) for  $b = 0.1$ ,  $\alpha = 0^\circ$ ,  $k_v = 0$  and  $N_c = 0.222$ ,  $M_c = N_c$

height of the wall ratio ( $L_r/H$ ) is going to be increased. For example, at  $\Phi = 25^\circ$ ,  $b = 0.1$ ,  $\alpha = 0^\circ$ ,  $N_c = 0.222$ ,  $M_c = N_c$  and  $k_v = k_h/2$  the increase in required length of reinforcement to height of the wall ratio ( $L_r/H$ ) is 19.5 % for  $k_h = 0.2$  over  $k_h = 0.1$ .

**2.3.9 Effect of Vertical Seismic Acceleration ( $k_v$ ) on Required Geo-synthetic Length**

The variation of required length of geosynthetic reinforcement to height of the wall ratio ( $L_r/H$ ) with respect to horizontal seismic acceleration ( $k_h$ ) at different vertical seismic acceleration ( $k_v$ ) for  $b = 0.1$ ,  $\alpha = 0^\circ$ ,  $\Phi = 20^\circ$  and  $N_c = 0.222$ ,  $M_c = N_c$  is shown in Fig. 12. From the plot, it is seen that the magnitude of the required length of geo-synthetic reinforcement to height of the wall ratio ( $L_r/H$ ) is going to be increased with the increase in vertical seismic acceleration ( $k_v$ ). For example, at  $\Phi = 20^\circ$ ,  $b = 0.1$ ,  $\alpha = 0^\circ$ ,  $k_h = 0.1$  and  $N_c = 0.222$ ,  $M_c = N_c$  the increase in required length of geo-synthetic reinforcement to height of the wall ratio ( $L_r/H$ ) is 0.93 % for  $k_v = 1.0 k_h$  over  $k_v = 0.0 k_h$ .

**2.3.10 Effect of Cohesion on Required Geo-synthetic Length**

The variation of required length of geo-synthetic reinforcement to height of the wall ratio ( $L_r/H$ ) with respect to soil friction angle ( $\Phi$ ) at different  $N_c$  value for  $b = 0.1$ ,  $\alpha = 0^\circ$ ,  $M_c = N_c$  and  $k_h = 0.2$ ,  $k_v =$

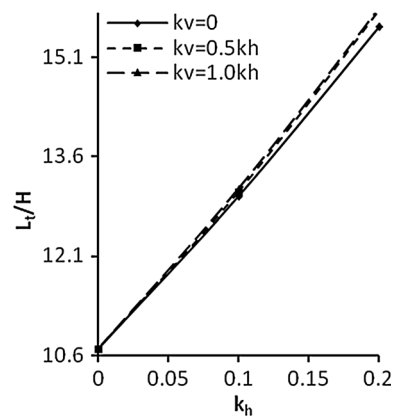


**Fig. 12** Variation of required length of geo-synthetic reinforcement to height of the wall ratio ( $L_r/H$ ) with respect to horizontal seismic acceleration ( $k_h$ ) at different vertical seismic acceleration ( $k_v$ ) for  $b = 0.1$ ,  $\alpha = 0^\circ$ ,  $\Phi = 20$  and  $N_c = 0.222$ ,  $M_c = N_c$



$k_h/2$  is shown in Fig. 13. From the plot it is seen that the magnitude of required length of geo-synthetic reinforcement to height of the wall ratio ( $L_t/H$ ) is going to be decreased due to the increase in  $N_c$  value. For example at  $\Phi = 20^\circ$ ,  $\alpha = 0^\circ$ ,  $M_c = N_c$  and  $k_h = 0.2$ ,  $k_v = k_h/2$ , the decrease in  $L_t/H$  is 33.47 % for  $N_c = 0.222$  over  $N_c = 0$  value whereas  $\Phi = 20^\circ$ ,  $\alpha = 0^\circ$ ,  $M_c = N_c$  and  $k_h = 0.2$ ,  $k_v = k_h/2$ , the decrease in  $L_t/H$  is 23.2 % for  $N_c = 0.1$  over  $N_c = 0$  value.

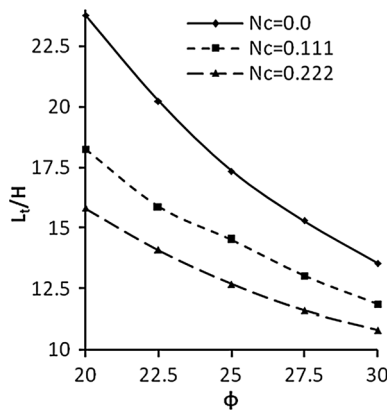


**Fig. 13** Variation of required length of geo-synthetic reinforcement to height of the wall ratio ( $L_t/H$ ) with respect to soil friction angle ( $\Phi$ ) at different  $N_c$  value for  $b = 0.1$ ,  $\alpha = 0^\circ$ ,  $M_c = N_c$  and  $k_h = 0.2$ ,  $k_v = k_h/2$

2.3.11 Effect of Non-linearity of the Failure Surface

The non-linearity of the failure surface at  $\Phi = 30^\circ$ ,  $N_c = 0.222$ ,  $M_c = N_c$  and  $k_h = 0.2$ ,  $k_v = k_h/2$  is shown in Fig. 14. From the plot it is seen that the nature of the failure surface is sagging in nature and it is most important in the evaluation for required length of geo-synthetic reinforcement for internal stability of reinforced earth retaining wall. The anchoring length of reinforcement should be extended beyond this zone. The required length of geo-synthetic reinforcement within the active zone increases with the increase in the degree of the non-linearity of failure surface. On the other hand, a consideration of linear failure surface provides less required length of reinforcements in comparison to the present analysis. So, this fact suggests the consideration of non-linear failure surface design in the case of reinforced earth retaining wall design.

2.3.12 Comparison of Results

The comparison of present results with pseudo-static results HSM by Shahgholi et al. (2001) and Ling et al. (1997) are presented in Table 1 considering  $\Phi$  soil as supporting backfill and cohesion value ( $c = 0$ ). From the comparison, it is seen that required tensile force is more or less same with Shahgholi et al. (2001). The comparison between present analysis and Mononobe-

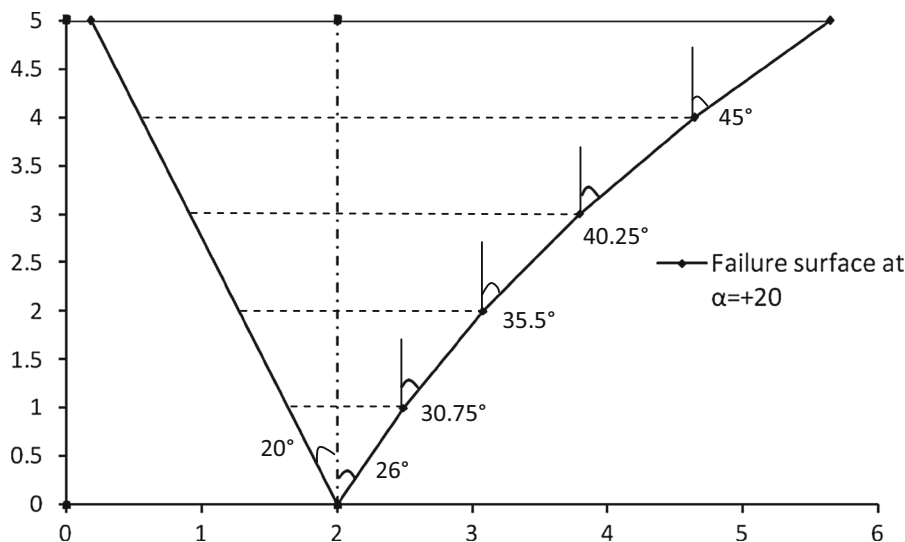


**Fig. 14** Non-linearity of the failure surface at  $\Phi = 30^\circ$ ,  $N_c = 0.222$ ,  $M_c = N_c$  and  $k_h = 0.2$ ,  $k_v = k_h/2$



**Table 1** Typical comparison of present results with Horizontal Slice Method of Shahgholi et al. (2001), and Ling et al. (1997) for  $k_v = 0.0$ ,  $H = 5$  m,  $\alpha = 0^\circ$  and  $N_c = 0$ ,  $M_c = 0$

$k_h$	Required geosynthetic reinforcement, $\sum t_i$ (kN/m)								
	$\Phi = 20^\circ$			$\Phi = 25^\circ$			$\Phi = 30^\circ$		
	Shahgholi et al. (2001)	Ling et al. (1997)	Present study	Shahgholi et al. (2001)	Ling et al. (1997)	Present study	Shahgholi et al. (2001)	Ling et al. (1997)	Present study
0.0	110	110	110	91	95	91	75	74	75
0.1	128	128	128	107	110	107	89	90	89
0.2	151	151	151	127	126	127	106	106	106
0.3	187	187	187	153	153	153	128	128	128

**Table 2** Typical comparison of present results with Mononobe-Okabe (Okabe 1926; Mononobe and Matsuo 1929) for  $H = 5$  m,  $\delta = \Phi/2$ ,  $\alpha = 0^\circ$  and  $N_c = 0$ ,  $M_c = 0$ ,  $k_h = 0.2$   $k_v = k_h/2$

$\Phi$	Present analysis		Mononobe-Okabe method (Okabe 1926; Mononobe and Matsuo 1929)	
	$k_a$	$\sum L_e$	$k_a$	$\sum L_e$
20	0.691	59.34	0.685	58.82
22.5	0.632	47.68	0.625	47.15
25	0.579	38.8	0.571	38.26
27.5	0.533	32.01	0.522	31.33
30	0.492	26.32	0.478	25.87

Okabe (Okabe 1926; Mononobe and Matsuo 1929) method is shown in Table 2 and it is seen that present method of analysis provides greater length of geosynthetic reinforcement in comparison to Mononobe-Okabe (Okabe 1926; Mononobe and Matsuo 1929).

### 3 Conclusions

In this paper, the seismic stability of reinforced soil wall system has been investigated using pseudo-static approach, with horizontal slice method of analysis considering non-linear failure surface. The effects of various parameters such as horizontal and vertical seismic accelerations, soil friction angle, cohesion, adhesion and wall inclination angle on the geosynthetic tensile reinforcement force and required length of the geo-synthetic reinforcement have been studied. The geo-synthetic tensile reinforcement force decreases with the increase in soil friction angle ( $\Phi$ ), cohesion ( $c$ ) and it increases with the increase in wall inclination angle and seismic accelerations. The present study also shows that the required length of geo-synthetic reinforcement increases due to increase

in wall inclination angle ( $\alpha$ ), seismic accelerations ( $k_h$ ,  $k_v$ ), and it decreases with the increase in soil friction angle ( $\Phi$ ), and cohesion value. The required length of geo-synthetic reinforcement is highly influenced by the degree of non-linearity of the failure surface and indicating that the actual inclination of the failure surface must be taken into account in the design of reinforced earth retaining wall.

### References

Ghosh S, Datta N (2012) Passive force on retaining wall supporting  $\Phi$  Backfill considering curvilinear rupture surface. *Int J Eng Invent* 1(10):35–42

Ghosh S, Saha A (2013) Non-linear rupture surface and response of retaining wall under static loading condition during active state of equilibrium. *Int J Emerg Technol Adv Eng* 3(6):509–515

Ghosh S, Saha A (2014) Non-linear failure surface and pseudodynamic passive resistance of a battered-faced retaining wall supporting  $c-\Phi$  backfill. *Int J Geomech ASCE* 14(3):1–9

Ling HI, Leshchinsky D (1998) Effects of vertical acceleration on seismic design of geo-synthetic-reinforced soil structures. *Geotechnique* 48(3):347–373

- Ling HI, Leshchinsky D, Perry EB (1997) Seismic design and performance of geo-synthetic reinforced soil structures. *Geotechnique* 47(5):933–952
- Mononobe N, Matsuo H (1929) On the determination of earth pressure during earthquakes. *Proc World Eng Conf* 9:177–185
- Nimbalkar SS, Choudhury D, Mandal JN (2006) Seismic stability of reinforced soil wall by pseudo-dynamic method. *Geo-synth Int* 13(3):111–119
- Nouri H, Fagher A, Jones CJFP (2008) Evaluating the effects of the magnitude and amplification of pseudo-static acceleration on reinforced soil slopes and walls using the limit equilibrium horizontal slices method. *Geotext Geomembr*, in press. doi:[10.1016/j.geotextmem.2007.09.002](https://doi.org/10.1016/j.geotextmem.2007.09.002)
- Okabe S (1926) General theory of earth pressure. *J Jpn Soc Civil Eng*, 12(1):1277–1323
- Shahgholi M, Fagher A, Joes CJFP (2001) Horizontal slice method of analysis. *Geotechnique* 51(10):881–885